

# CP/MAS NMR of Heavy Spin-1/2 Nuclei at $B_0 = 2.35$ T

Frank Ambrosius, Elke Klaus, Torsten Schaller, and Angelika Sebald  
Bayerisches Geoinstitut, Universität Bayreuth, D-95440 Bayreuth

Z. Naturforsch. **50a**, 423–428 (1995); received November 8, 1994

*Dedicated to Prof. W. Müller-Warmuth on the occasion of his 65th birthday*

Perspectives of CP/MAS NMR at low external magnetic field ( $B_0 = 2.35$  T) are discussed. Applications are illustrated for the case of heavy spin-1/2 nuclei such as  $^{195}\text{Pt}$  and  $^{199}\text{Hg}$ .  $^{195}\text{Pt}$  and  $^{199}\text{Hg}$  CP/MAS spectra of a variety of organometallic compounds are reported. Aspects of shielding anisotropies, of  $^{195}\text{Pt}$ - $^{35/37}\text{Cl}$  interactions and of  $^{31}\text{P}$ -M (M = Cd, Hg, Pt) coupling in transition metal phosphine complexes will be briefly addressed.

**Key words:** High-resolution solid-state NMR, cross polarisation, magic angle spinning,  $^{195}\text{Pt}$ ,  $^{199}\text{Hg}$ .

## Introduction

When dealing with NMR of solutions, mainly reasons of sensitivity and resolution recommend operation at high  $B_0$ . In the case of high-resolution solid-state NMR, the optimum  $B_0$  depends on the nature of the respective area of application. In high-resolution solid-state NMR only single pulse magic angle spinning (MAS) experiments on quadrupolar nuclei gain from the use of very high magnetic fields  $B_0$  – if a reduction of second order quadrupole interactions is intended. The most commonly used spin-1/2 nuclei in high-resolution solid-state NMR are  $^{13}\text{C}$ ,  $^{29}\text{Si}$ , and  $^{31}\text{P}$ , and very often double-resonance methods (cross polarisation (CP)) are the method of choice to create observable magnetisation. The properties of these nuclei in a large variety of chemicals are such that MAS and CP/MAS experiments at medium to high  $B_0$  ( $B_0 = 4.7$ – $11.5$  T) are the most efficient compromise: increased sensitivity and chemical shift resolution at higher fields is counterbalanced by increasingly expressed spinning sideband patterns due to chemical shift anisotropy. Accordingly, the most widely used magnetic field strengths for MAS and CP/MAS applications are in the range  $B_0 = 4.7$ – $11.5$  T.

Several circumstances, favouring the use of low external magnetic field strengths for MAS and CP/MAS NMR come to mind. Suppose “spin-counting”, that is quantitation of MAS spectra, is aimed at for nuclei such as  $^{13}\text{C}$ ,  $^{29}\text{Si}$ ,  $^{31}\text{P}$ . Often, at low  $B_0$ , modest MAS frequencies can then yield completely isotropic spectra, free of spinning sidebands. A practical application

for such purposes in the case of  $^{13}\text{C}$  have been MAS (and CP/MAS) investigations of coals and organic soil matter [1, 2]. Also for the investigation of solid-state dynamics of organic and organometallic compounds by means of  $^{13}\text{C}$  CP/MAS, this easily achievable “fast spinning regime” (that is  $v_{\text{rot}}$  exceeds the width of the  $^{13}\text{C}$  chemical shielding anisotropy (csa) pattern) can be an advantage: existing solution-state NMR methodology can then be directly applied for the solid state. Furthermore, in a slow chemical exchange regime, where the  $^{13}\text{C}$  chemical shift scale defines the NMR time-scale to monitor the exchange process by one-dimensional variable-temperature  $^{13}\text{C}$  CP/MAS, a low  $B_0$  can be helpful, given that such compounds are often not particularly stable at elevated temperatures. Operating at lower  $B_0$  can be viewed as equivalent to a fictitious temperature change to “higher” temperatures. Suppose that cross polarisation experiments utilising nuclei other than  $^1\text{H}$  as the source of magnetisation is the desired mode of operation. Again, low  $B_0$  can be useful since abundant nuclei such as  $^{19}\text{F}$  or  $^{31}\text{P}$  (potential sources of magnetisation) will there show favourable characteristics for Hartmann-Hahn cross polarisation. Also, the study of the effects of neighbouring quadrupolar nuclei ( $^{14}\text{N}$ ,  $^{35/37}\text{Cl}$ ) on the MAS spectra of spin-1/2 nuclei may require the use of low magnetic field strengths in addition to work at higher fields [3]. Finally, heavy spin-1/2 nuclei such as  $^{195}\text{Pt}$  or  $^{199}\text{Hg}$  will usually display enormous chemical shielding anisotropies (csa) of the order of up to several thousand ppm. Such csa values have so far almost completely prevented the use of these nuclei in CP/MAS NMR studies at more common magnetic field strengths  $B_0 = 4.7$ – $9.4$  T [4].

Reprint requests to Dr. Angelika Sebald.

0932-0784 / 95 / 0400-0423 \$ 06.00 © – Verlag der Zeitschrift für Naturforschung, D-72027 Tübingen



Dieses Werk wurde im Jahr 2013 vom Verlag Zeitschrift für Naturforschung in Zusammenarbeit mit der Max-Planck-Gesellschaft zur Förderung der Wissenschaften e.V. digitalisiert und unter folgender Lizenz veröffentlicht: Creative Commons Namensnennung-Keine Bearbeitung 3.0 Deutschland Lizenz.

Zum 01.01.2015 ist eine Anpassung der Lizenzbedingungen (Entfall der Creative Commons Lizenzbedingung „Keine Bearbeitung“) beabsichtigt, um eine Nachnutzung auch im Rahmen zukünftiger wissenschaftlicher Nutzungsformen zu ermöglichen.

This work has been digitalized and published in 2013 by Verlag Zeitschrift für Naturforschung in cooperation with the Max Planck Society for the Advancement of Science under a Creative Commons Attribution-NoDerivs 3.0 Germany License.

On 01.01.2015 it is planned to change the License Conditions (the removal of the Creative Commons License condition “no derivative works”). This is to allow reuse in the area of future scientific usage.

In the following we will illustrate that an external magnetic field  $B_0 = 2.35$  T can overcome such large-csa-related problems for  $^{195}\text{Pt}$ ,  $^{199}\text{Hg}$  (and other, similar cases). "Small" can be quite powerful!

## Experimental

All CP/MAS experiments have been carried out using a Bruker MSL 100 NMR spectrometer, equipped with a standard broad-banded double-bearing CP/MAS probe.  $^1\text{H}$  90° pulse durations were 4–5  $\mu\text{s}$ , CP contact times typically were in the range 3–8 ms. MAS frequencies, relaxation delays and number of accumulated transients are given in the respective figure captions.  $\text{Cd}(\text{NO}_3)_2 \cdot 4\text{H}_2\text{O}$  ( $^{113}\text{Cd}$ ),  $\text{Hg}(\text{OAc})_2$  ( $^{199}\text{Hg}$ ) and  $\text{K}_2\text{Pt}(\text{OH})_6$  ( $^{195}\text{Pt}$ ) were used to set the Hartmann-Hahn matching condition, isotropic chemical shifts are quoted with respect to  $\text{H}_3\text{PO}_4$  ( $^{31}\text{P}$ ),  $\Xi^{195}\text{Pt} = 21.4$  MHz ( $^{195}\text{Pt}$ ), neat  $\text{HgMe}_2$  ( $^{199}\text{Hg}$ ) and 1 M  $\text{Cd}(\text{ClO}_4)_2$  in  $\text{H}_2\text{O}$  ( $^{113}\text{Cd}$ ) [4].

All compounds used in this study are either commercially available or can be synthesized by routine preparative methods.

## Results and Discussion

Our  $^{113}\text{Cd}$ ,  $^{195}\text{Pt}$  and  $^{199}\text{Hg}$  CP/MAS results are illustrated in Fig. 1–5, isotropic chemical shifts, scalar coupling constants  $J$  and, where appropriate, shielding tensor components are given in Table 1.

We will first consider the nucleus  $^{195}\text{Pt}$ . While representing a well-established solution-state NMR probe [5],  $^{195}\text{Pt}$  has scarcely been established as a high-resolution solid state NMR probe. Of the few  $^{195}\text{Pt}$  CP/MAS studies to be found in the literature, the majority is concerned with Pt(IV) in octahedral coordination. The more common formal oxidation state Pt(II) with Pt in square-planar coordination has to date not been considered widely [4]. This is by no means surprising, given that for Pt(II) in its typical coordination,  $^{195}\text{Pt}$  shielding tensor patterns of 3000–10 000 ppm width are to be expected. Pt(IV) in octahedral, or nearly octahedral coordination gives rise to much less expressed  $^{195}\text{Pt}$  shielding patterns, which are more easily manageable at higher external magnetic field strengths  $B_0$ . Even minor distortions from regular octahedral symmetry still yield  $^{195}\text{Pt}$  csa patterns covering several hundred ppm. This is illustrated in Fig. 1 where  $^{195}\text{Pt}$  CP/MAS spectra of  $\text{K}_2\text{Pt}(\text{OH})_6$  at  $B_0 = 2.35$  T and  $B_0 = 7$  T are compared.  $\text{K}_2\text{Pt}(\text{OH})_6$  serves as a convenient set-up compound for  $^{195}\text{Pt}$  CP/MAS studies. At  $B_0 = 2.35$  T the Hartmann-Hahn matching condition can be optimised on this compound from the single transient  $^{195}\text{Pt}$  CP/MAS response.

Figure 2 shows the 21.4 MHz  $^{195}\text{Pt}$  CP/MAS spectrum of  $(\text{Ph}_3\text{P})_2\text{Pt}(\text{C}_2\text{H}_4)$ , representing a fairly unusual case, as this spectrum is virtually free of spinning sidebands. It has been noted [6] that the fragment *cis*- $\text{P}_2\text{PtC}_2$  generally displays narrow  $^{195}\text{Pt}$  csa patterns, irrespective of the formal oxidation state of plat-

Table 1.  $^{31}\text{P}$ -,  $^{113}\text{Cd}$ -,  $^{195}\text{Pt}$ -, and  $^{199}\text{Hg}$ -NMR data.

Compound	M	$\delta_{\text{iso}} \text{M}$ [ppm]	shielding tensor components $\text{M}^a$				$\delta_{\text{iso}} ^{31}\text{P}$ [ppm]	$^1J(\text{M}^{31}\text{P})^b$ [Hz]
			$\sigma_{11}$	$\sigma_{22}$	$\sigma_{33}$	$\eta$		
$\text{K}_2\text{Pt}(\text{OH})_6$	$^{195}\text{Pt}$	+8024						
		+7998 <sup>c</sup>	−8165	−8089	−7740	0.3		
$(\text{Ph}_3\text{P})_2\text{Pt}(\text{C}_2\text{H}_4)^d$	$^{195}\text{Pt}$	−496					31.1 36.7	3772 3656
$\text{CODPtCl}_2$	$^{195}\text{Pt}$	+1177	1229	311	−5071	0.2		
<i>cis</i> -( $\text{Et}_2\text{S}$ ) $_2\text{PtCl}_2$	$^{195}\text{Pt}$	+877	1507	358	−4496	0.3		
<i>trans</i> -( $\text{Et}_2\text{S}$ ) $_2\text{PtCl}_2$	$^{195}\text{Pt}$	+1101	1408	226	−4997	0.3		
<i>trans</i> -( $^n\text{Bu}_3\text{P}$ ) $_2\text{PtCl}_2$ <sup>e</sup>	$^{195}\text{Pt}$	+607					5.6	2414
$\text{Hg}(\text{OAc})_2$	$^{199}\text{Hg}$	−2490	1897	1907	3666	0.0		
$\text{Ph-Hg-OAc}$	$^{199}\text{Hg}$	−1499	187	375	3935	0.1		
$\text{HgPh}_2$	$^{199}\text{Hg}$	−829	−1122	−699	4307	0.1		
$\text{Hg}(\text{OAc})_2 \cdot \text{Pchex}_3$	$^{199}\text{Hg}$	−1149					59.9	8226
$\text{Cd}(\text{ClO}_4)_2 \cdot 2\text{Pchex}_3$	$^{113}\text{Cd}$	+283					39.3 30.8	2305 2150

<sup>a</sup> Haeberlen's notation [17] is used to report shielding tensor components;  $\sigma_{\text{iso}} = -\delta_{\text{iso}}$ ;  $|\sigma_{33} - \sigma_{\text{iso}}| \geq |\sigma_{11} - \sigma_{\text{iso}}| \geq |\sigma_{22} - \sigma_{\text{iso}}|$ ;  $\eta = (\sigma_{22} - \sigma_{11}) / (\sigma_{33} - \sigma_{\text{iso}})^{-1}$ . <sup>b</sup> determined from  $^{31}\text{P}$  CP/MAS spectra and from  $^{113}\text{Cd}$ ,  $^{195}\text{Pt}$ ,  $^{199}\text{Hg}$  CP/MAS spectra. <sup>c</sup> data taken from [18] and converted to  $\Xi^{195}\text{Pt} = 21.4$  MHz. <sup>d</sup> see also [6]. <sup>e</sup>  $^{31}\text{P}$  data taken from [16].

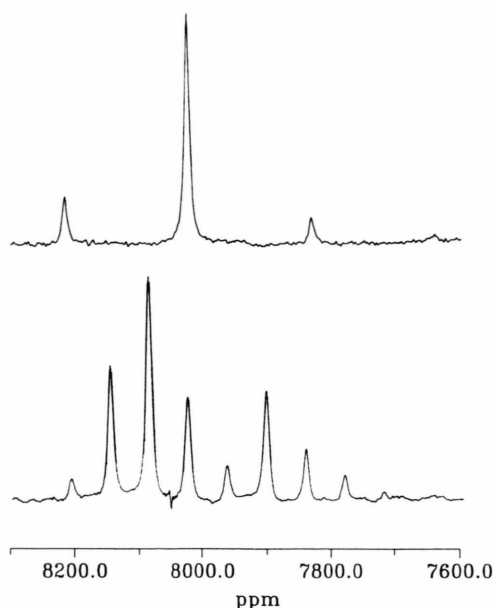


Fig. 1.  $^{195}\text{Pt}$  CP/MAS spectra of  $\text{K}_2\text{Pt}(\text{OH})_6$  at 21.4 MHz (top) and 64.2 MHz (bottom). Both spectra are the result of 160 transients and a recycle delay of 4 s. MAS frequencies were 4.1 kHz (top) and 4 kHz (bottom).

inum (Pt(0), Pt(II)) and the formal hybridisation of carbon ( $\text{sp}$ ,  $\text{sp}^2$ ,  $\text{sp}^3$ ).

In contrast to the 64.2 MHz  $^{195}\text{Pt}$  CP/MAS spectrum of  $(\text{Ph}_3\text{P})_2\text{Pt}(\text{C}_2\text{H}_4)$  [6], the 21.4 MHz spectrum clearly resolves scalar coupling  $^1J(^{195}\text{Pt}^{31}\text{P})$  to two inequivalent  $^{31}\text{P}$  nuclei. The finding of modest  $^{195}\text{Pt}$  csa patterns for the *cis*- $\text{P}_2\text{PtC}_2$  fragment is relevant from a chemical point of view: the  $\text{P}_2\text{PtC}_2$  fragment plays an important role in platinum coordination-complex chemistry and, therefore, is an important target for  $^{195}\text{Pt}$  CP/MAS studies.

Platinum(II)-compounds such as  $\text{CODPtCl}_2$  (COD = cyclooctadiene) and *cis*- and *trans*-( $\text{Et}_2\text{S}$ ) $_2\text{PtCl}_2$  are widely used starting materials in platinum chemistry, ligands such as COD,  $\text{Et}_2\text{S}$  can easily be replaced by other ligands such as phosphines  $\text{PR}_3$ . 21.4 MHz  $^{195}\text{Pt}$  CP/MAS spectra of these three compounds are shown in Figure 3. The spinning sideband patterns observed for these compounds are quite representative for what has to be expected for Pt(II) in compounds  $\text{L}_2\text{PtX}_2$ . The patterns cover a range of approximately 6000 ppm (see Table 1) and the  $^{195}\text{Pt}$  shielding tensors are not axially symmetric. Note that the principal shielding tensor components for *cis*- and *trans*-( $\text{Et}_2\text{S}$ ) $_2\text{PtCl}_2$  do not allow assignment of the respective *cis*- or *trans*-isomer. This will be generally true for  $^{195}\text{Pt}$  in square-planar  $\text{L}_2\text{PtX}_2$  coordination on the grounds of molecular symmetry. Both (idealised)  $\text{C}_{2v}$  symmetry for *cis*-isomers and  $\text{D}_{2h}$  symmetry for *trans*-isomers do not require axially symmetric  $^{195}\text{Pt}$  shielding tensors, nor is the assignment of the individual principal components  $\sigma_{11}$ ,  $\sigma_{22}$ ,  $\sigma_{33}$  in the molecular axes system uniquely prescribed by the molecular point group symmetry. Furthermore, the  $^{195}\text{Pt}$  CP/MAS spectra of  $\text{CODPtCl}_2$ , *cis*- and *trans*-( $\text{Et}_2\text{S}$ ) $_2\text{PtCl}_2$  (and, in fact, of further Pt(II) compounds  $\text{L}_2\text{PtCl}_2$ ) seemingly lack the complexity of considerable broadening and/or splitting due to quadrupolar and scalar couplings  $^{195}\text{Pt}$ - $^{35/37}\text{Cl}$ . This finding is in marked contrast to  $^{195}\text{Pt}$  MAS spectra of  $\text{PtCl}_6^{2-}$  salts [7] where complex lineshapes, caused by  $^{195}\text{Pt}$ - $^{35/37}\text{Cl}$  interactions, have been observed and analysed. The detectability of second-order quadrupolar effects in the spectra of a neighboured spin-1/2 nucleus requires sufficiently slow  $T_1$ -relaxation of the quadrupolar nucleus. Hence, it would appear reasonable to ascribe the lack of complexity in these three  $^{195}\text{Pt}$  CP/MAS spectra (Fig. 3) to “self-decoupling” [3] brought about

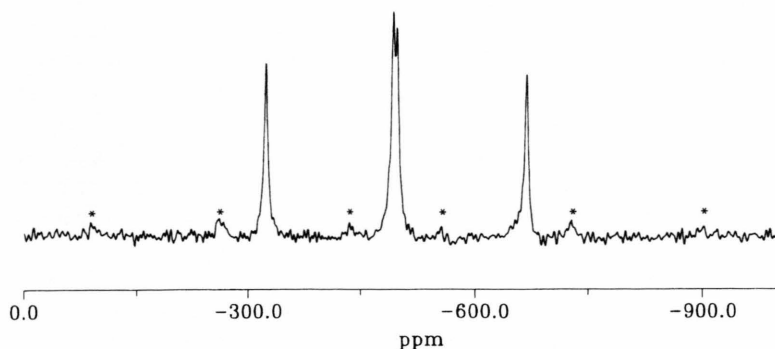


Fig. 2. 21.4 MHz  $^{195}\text{Pt}$  CP/MAS of  $(\text{Ph}_3\text{P})_2\text{Pt}(\text{C}_2\text{H}_4)$ :  $\nu_{\text{rot}} = 5$  kHz, recycle delay 6 s, contact time 6 ms, 4110 transients. The splitting due to  $^1J(^{195}\text{Pt}^{31}\text{P})$  with two inequivalent  $^{31}\text{P}$  nuclei is clearly resolved, \* mark residual spinning sidebands.

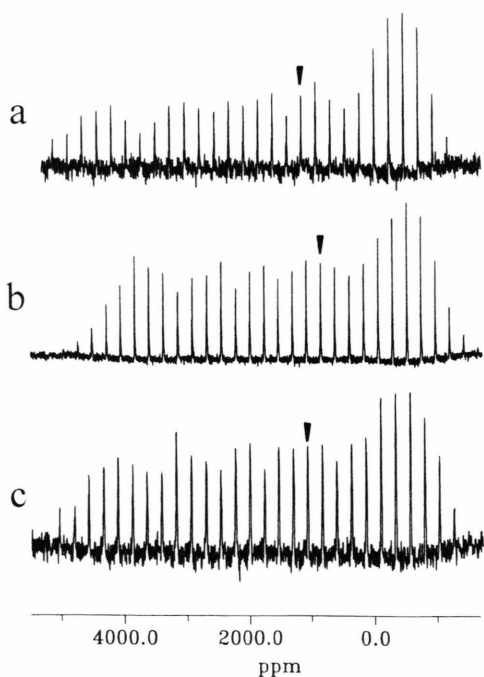


Fig. 3. 21.4 MHz  $^{195}\text{Pt}$  CP/MAS of a)  $\text{CODPtCl}_2$ , b)  $\text{cis}-(\text{Et}_2\text{S})_2\text{PtCl}_2$ , c)  $\text{trans}-(\text{Et}_2\text{S})_2\text{PtCl}_2$ . Centre bands are marked by ▼. a)  $\nu_{\text{rot}} = 5$  kHz, recycle delay 3 s, contact time 5 ms, 9400 transients, b)  $\nu_{\text{rot}} = 4.9$  kHz, recycle delay 3 s, contact time 5 ms, 15 450 transients, c)  $\nu_{\text{rot}} = 5$  kHz, recycle delay 3 s, contact time 5 ms, 4000 transients.

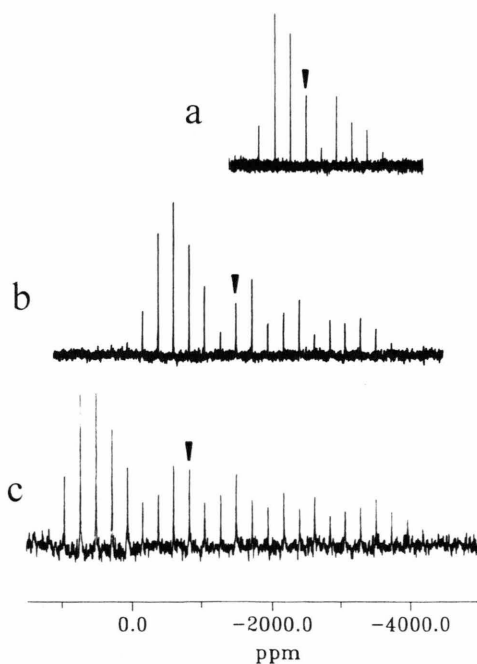


Fig. 4. 17.9 MHz  $^{199}\text{Hg}$  CP/MAS of a)  $\text{Hg}(\text{OAc})_2$ , b)  $\text{Ph-Hg-OAc}$ , c)  $\text{HgPh}_2$ ;  $\nu_{\text{rot}} = 4$  kHz, contact times 5 ms, ▼ denotes centre bands. a) recycle delay 4 s, 800 transients, b) recycle delay 60 s, 1500 transients, c) recycle delay 60 s, 2400 transients.

by fast  $^{35/37}\text{Cl}$   $T_1$ -relaxation. However, the widths at half-height ( $\nu_{1/2} = 250$  Hz) of the various spinning sidebands in the 21.4 MHz  $^{195}\text{Pt}$  CP/MAS spectrum of  $\text{CODPtCl}_2$  are greater than in the corresponding 64.2 MHz  $^{195}\text{Pt}$  CP/MAS spectrum ( $\nu_{1/2} = 150$  Hz). The lineshape of these  $^{195}\text{Pt}$  resonances depends on the ratio of quadrupole to Zeeman frequencies of the neighboured chlorine nuclei and, thus, complete  $^{195}\text{Pt}$ - $^{35/37}\text{Cl}$  self-decoupling can be ruled out for these  $\text{L}_2\text{PtCl}_2$  complexes. Clearly, more work will be necessary to characterise the  $^{195}\text{Pt}$ - $^{35/37}\text{Cl}$  interactions in the  $\text{Cl}_2\text{Pt}$  fragment in *cis*- and *trans*- $\text{L}_2\text{PtCl}_2$  complexes. Again, as in the case of the  $\text{P}_2\text{Pt}_2$  fragment, the motivation is promoted by the chemical importance of the  $\text{Cl}_2\text{Pt}$  fragment.

Let us next consider some examples of  $^{199}\text{Hg}$  CP/MAS spectra obtained at  $B_0 = 2.35$  T. Similar to the case of  $^{195}\text{Pt}$ ,  $^{199}\text{Hg}$  csa patterns of several thousand ppm width have so far almost completely prevented the use of this nucleus in high-resolution solid-state NMR [4]. Other than for  $^{195}\text{Pt}$ , in addition solution-

state  $^{199}\text{Hg}$  NMR spectroscopy often suffers from fast chemical exchange of ligands in solution, so that  $^{199}\text{Hg}$  CP/MAS NMR of polycrystalline samples could provide a quasi-slow exchange regime for such cases. Figure 4 shows the 17.9 MHz  $^{199}\text{Hg}$  CP/MAS spectra of a series of compounds  $\text{Hg}(\text{OAc})_2$ ,  $\text{Ph-Hg-OAc}$ ,  $\text{HgPh}_2$ .

On going from  $\text{Hg}(\text{OAc})_2$  to  $\text{HgPh}_2$  we note a dramatic increase in the width of the  $^{199}\text{Hg}$  shielding tensor pattern, starting with  $\Delta\sigma \approx 2000$  ppm for  $\text{Hg}(\text{OAc})_2$  and ending with  $\Delta\sigma \approx 5500$  ppm for  $\text{HgPh}_2$ . Such an increase is in accord with the respective chemical environment in this series of compounds. While mercury in solid  $\text{Hg}(\text{OAc})_2$  may be described as residing in an extremely strongly distorted  $\text{HgO}_4$  coordination, the mercury environment in  $\text{HgPh}_2$  is a linear two-fold  $\text{HgC}_2$  coordination.  $^{199}\text{Hg}$  shielding anisotropies in organomercury compound such as  $\text{HgMe}_2$  [8–11],  $\text{MeHgX}$  ( $\text{X} = \text{Cl}, \text{Br}, \text{I}$ ) [8] and  $\text{HgPh}_2$  [12, 13] have in the past been investigated by means of NMR experiments in nematic and



smectic liquid crystal solvents and by  $^{199}\text{Hg}$   $T_1$  relaxation measurements in isotropic solutions at high magnetic field strengths. For  $\text{HgPh}_2$  it was found that at high fields  $^{199}\text{Hg}$  relaxation is completely dominated by the csa-relaxation mechanism. From  $^{199}\text{Hg}$   $T_1$  data for  $\text{HgPh}_2$   $\Delta\sigma(^{199}\text{Hg}) = 5800 \pm 600$  ppm [12] and  $\Delta\sigma(^{199}\text{Hg}) = 6800 \pm 680$  ppm [13] have been calculated. These solution-state NMR results are confirmed by the  $^{199}\text{Hg}$  CP/MAS spectrum of  $\text{HgPh}_2$  (see Fig. 4 and Table 1, for  $\text{HgPh}_2$   $\Delta\sigma = \sigma_{33} - \sigma_{11} = 5429$  ppm from  $^{199}\text{Hg}$  CP/MAS).

Finally, some representative examples of  $^{113}\text{Cd}$ ,  $^{195}\text{Pt}$  and  $^{199}\text{Hg}$  CP/MAS spectra of transition metal phosphine complexes  $\text{MX}_2 \cdot \text{PR}_3$ ,  $\text{MX}_2 \cdot 2\text{PR}_3$  are illustrated in Figure 5. In solution at ambient temperatures cadmium- and mercury-phosphine complexes  $\text{MX}_2 \cdot \text{PR}_3$ ,  $\text{MX}_2 \cdot 2\text{PR}_3$  ( $\text{M} = \text{Cd}, \text{Hg}$ ) tend to undergo fast chemical exchange of phosphine ligands  $\text{PR}_3$ . No such chemical exchange occurs in the solid state and crystalline complexes of various  $\text{M}:\text{PR}_3$  stoichiometries can be isolated. Two typical such compounds are  $\text{Cd}(\text{ClO}_4)_2 \cdot 2\text{Pchex}_3$  ( $\text{chex} = \text{cyclohexyl}$ ) and  $\text{Hg}(\text{OAc})_2 \cdot \text{Pchex}_3$ , the  $^{113}\text{Cd}$  and  $^{199}\text{Hg}$  CP/MAS spectra of which are shown in Figure 5a, b. The two  $\text{Pchex}_3$  ligands in solid crystalline  $\text{Cd}(\text{ClO}_4)_2 \cdot 2\text{Pchex}_3$  are crystallographically inequivalent, display different  $^{31}\text{P}$  chemical shifts ( $\delta^{31}\text{P} = 30.8$  and  $39.3$  ppm) and different coupling constants  $^1J(^{113}\text{Cd}^{31}\text{P})$  (2150 Hz and 2305 Hz, respectively). Accordingly, the  $^{113}\text{Cd}$  CP/MAS resonance is split into a doublet of doublets as indicated in Figure 5a. The  $^{199}\text{Hg}$  CP/MAS spectrum of  $\text{Hg}(\text{OAc})_2 \cdot \text{Pchex}_3$  (see Fig. 5b) is characterised by a large splitting  $^1J(^{199}\text{Hg}^{31}\text{P}) = 8226$  Hz. In both cases it is straightforward to obtain isotropic data  $\delta\text{M}$ ,  $\delta^{31}\text{P}$ ,  $^1J(\text{M}^{31}\text{P})$  from CP/MAS spectra. Owing to the simultaneous presence of shielding anisotropy, anisotropic  $J$ -coupling and dipolar interactions it is, however, much less straightforward to obtain information on these anisotropic interactions from simple CP/MAS spectra if no undue assumption about relative orientations and asymmetries are to be made. In particular for cases with low molecular symmetry such as  $\text{Cd}(\text{ClO}_4)_2 \cdot 2\text{Pchex}_3$  or  $\text{Hg}(\text{OAc})_2 \cdot \text{Pchex}_3$ , analysis of anisotropic interactions within the  $\text{M}-^{31}\text{P}$  spin pair or  $\text{M}(^{31}\text{P})_2$  ABX spin system from powder spectra requires considerable computational efforts and/or the use of more sophisticated MAS NMR experiments [14a]. Alternatively, single-crystal NMR methods may be employed to directly obtain such information [14b]. It is important

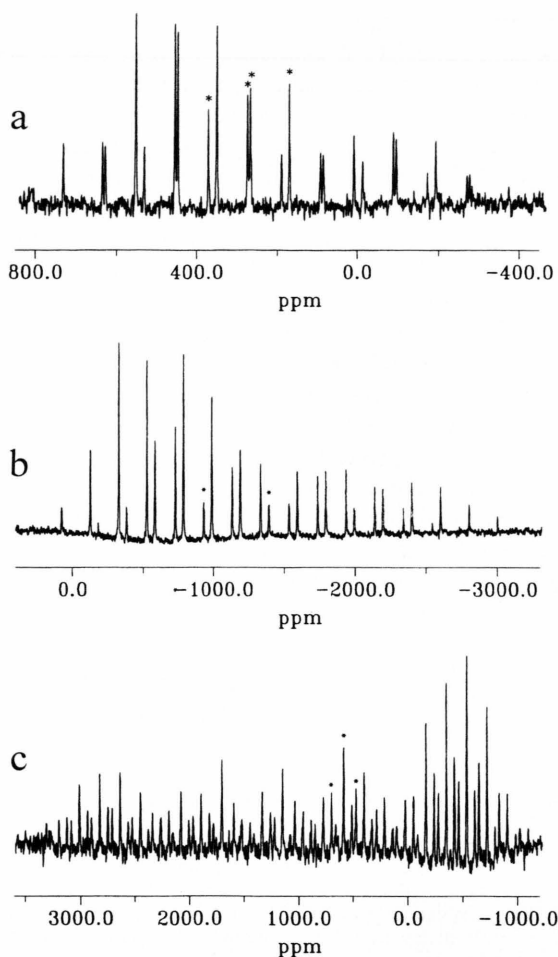


Fig. 5.  $^{113}\text{Cd}$  (22.2 MHz),  $^{199}\text{Hg}$  (17.9 MHz) and  $^{195}\text{Pt}$  (21.4 MHz) CP/MAS of transition metal phosphine complexes, centre bands and isotropic  $J$  coupling  $^1J(\text{M}^{31}\text{P})$  ( $\text{M} = ^{113}\text{Cd}$ ,  $^{199}\text{Hg}$ ,  $^{195}\text{Pt}$ ) are marked by \*. a)  $^{113}\text{Cd}$  CP/MAS of  $\text{Cd}(\text{ClO}_4)_2 \cdot 2\text{Pchex}_3$  ( $\text{chex} = \text{cyclohexyl}$ ),  $\nu_{\text{rot}} = 4$  kHz, contact time 5 ms, recycle delay 3 s, 8400 transients. Note coupling  $^1J(^{113}\text{Cd}^{31}\text{P})$  with two inequivalent  $^{31}\text{P}$  nuclei. – b)  $^{199}\text{Hg}$  CP/MAS of  $\text{Hg}(\text{OAc})_2 \cdot \text{Pchex}_3$ ,  $\nu_{\text{rot}} = 3.6$  kHz, contact time 5 ms, recycle delay 3 s, 21 500 transients. – c)  $^{195}\text{Pt}$  CP/MAS of  $\text{trans}-(\text{nBu}_3\text{P})_2\text{PtCl}_2$ ,  $\nu_{\text{rot}} = 4$  kHz, contact time 5 ms, recycle delay 4 s, 10 600 transients.

that we learn in more detailed about anisotropic interactions within such  $\text{M}-^{31}\text{P}$ ,  $\text{M}(^{31}\text{P})_2$  systems because  $^{31}\text{P}$  CP/MAS NMR is already a routine method for the characterisation of transition metal phosphine complexes, CP/MAS NMR of nuclei such as  $^{113}\text{Cd}$ ,  $^{195}\text{Pt}$ ,  $^{199}\text{Hg}$  is on its way to become routinely available. The absence of more precise knowledge about such solid-state two- and three-spin systems is danger-

ous with respect to possible mis- or over-interpretation of routine CP/MAS spectra. Efforts towards a more detailed understanding of the homonuclear  $^{31}\text{P}$  spin pair in cadmium- and mercury-phosphine complexes  $\text{MX}_2 \cdot 2\text{PR}_3$  under MAS conditions have recently been described [15]. Another typical example of a  $\text{M}(^{31}\text{P})_2$  spin system is the platinum(II) complex *trans*-( $^n\text{Bu}_3\text{P}$ ) $_2\text{PtCl}_2$  (the  $^{195}\text{Pt}$  CP/MAS spectrum is depicted in Figure 5c). Clearly, at 21.4 MHz  $^{195}\text{Pt}$  shielding anisotropy is still the overwhelming spectral parameter but there are also indications of residual broadening caused by  $^{195}\text{Pt}$ - $^{35/37}\text{Cl}$  interactions as well as splittings caused by  $^1\text{J}(^{195}\text{Pt}^{31}\text{P})$ . The two  $^{31}\text{P}$  nuclei in *trans*-( $^n\text{Bu}_3\text{P}$ ) $_2\text{PtCl}_2$  are chemically equivalent, but not magnetically equivalent (that is the two  $^{31}\text{P}$  shielding tensors are not connected by a centre of inversion as an applicable symmetry operation) and, hence, the  $^{31}\text{P}$  CP/MAS spectra of *trans*-( $^n\text{Bu}_3\text{P}$ ) $_2\text{PtCl}_2$  display MAS frequency (and  $B_0$ ) dependent second order effects ("J-recoupling") [16] which, under appropriate conditions, will also render the  $^{195}\text{Pt}$  CP/MAS spectrum homogeneous [14, 19].

In summary, the  $^{113}\text{Cd}$ ,  $^{195}\text{Pt}$  and  $^{199}\text{Hg}$  CP/MAS spectra in Fig. 5 reflect the ease with which, at low  $B_0$ , such spectra may be obtained. Likewise, these spectra also demonstrate the degree of complexity which spin systems  $\text{M}-^{31}\text{P}$ ,  $\text{M}(^{31}\text{P})_2$  ( $\text{M} = ^{113}\text{Cd}$ ,  $^{195}\text{Pt}$ ,  $^{199}\text{Hg}$ ) under MAS will represent in many cases.

To conclude, we would like to emphasize once more the considerable degree of experimental freedom to be gained for MAS and CP/MAS NMR if the use of fairly low external magnetic field strengths is included: loss of sensitivity is not the crucial issue, even if sensitivity considerations cannot be completely disregarded.

#### Acknowledgements

Generous support of our work by the Deutsche Forschungsgemeinschaft and the Fonds der Chemischen Industrie is gratefully acknowledged. We thank DEGUSSA AG, Hanau, for their loan of precious metal salts.

- [1] a) C. E. Snape, D. E. Axelson, R. E. Botto, J.-J. Delpuech, P. Tekeley, B. C. Gerstein, M. Pruski, G. E. Maciel, and M. A. Wilson, *Fuel* **68**, 547 (1987); b) W. Meiler and R. Meusinger; *Ann. Reports NMR Spectrosc.* **24**, 331 (1992), (ed. G. A. Webb) Academic Press, London.
- [2] M. A. Wilson, *NMR Techniques and Applications in Geochemistry and Soil Chemistry*, Pergamon Press, Oxford 1987.
- [3] R. K. Harris and A. C. Olivieri, *Progr. in NMR Spectrosc.* **24**, 435 (1992).
- [4] A. Sebald, *NMR Basic Principles and Progress* **31**, 91 (1994).
- [5] P. S. Pregosin, in: P. S. Pregosin (ed.): *Transition Metal Nuclear Magnetic Resonance (Studies in Inorg. Chem. Vol. 13)*, Elsevier, Amsterdam 1991, p. 216.
- [6] R. Challoner and A. Sebald, *Solid State NMR*, **4**, 39 (1995).
- [7] S. Hayashi and K. Hayamizu, *Magn. Reson. Chem.* **30**, 658 (1992).
- [8] J. D. Kennedy and W. McFarlane, *J. Chem. Soc. Faraday Trans. II* **72**, 1653 (1976).
- [9] J. Jokisaari and P. Diehl, *Org. Magn. Reson.* **13**, 359 (1980).
- [10] J. Jokisaari and K. Räsänen, *Mol. Phys.* **36**, 113 (1978).
- [11] C. R. Lassigne and E. J. Wells, *Can. J. Chem.* **55**, 1303 (1977).
- [12] R. E. Wasylshen, R. E. Lenkinski, and C. Rodger; *Can. J. Chem.* **60**, 2113 (1982).
- [13] D. C. Gillies, L. P. Blaauw, G. R. Hays, R. Huis, and A. D. H. Clague, *J. Magn. Reson.* **42**, 420 (1981).
- [14] a) R. Challoner and C. A. McDowell, *J. Magn. Reson.* **98**, 123 (1992). b) M. D. Lumsden, K. Eichele, R. E. Wasylshen, T. S. Cameron, and J. F. Britten, *J. Amer. Chem. Soc.* **116**, 11129 (1994).
- [15] a) G. Wu and R. E. Wasylshen, *J. Chem. Phys.* **98**, 6138 (1993); b) G. Wu and R. E. Wasylshen, *J. Chem. Phys.* **100**, 4828 (1994); c) G. Wu and R. E. Wasylshen, *J. Chem. Phys.* **100**, 5546 (1994); d) K. Eichele, G. Wu, and R. E. Wasylshen; *J. Magn. Reson. A* **101**, 157 (1993).
- [16] E. Klaus and A. Sebald; *Angew. Chemie*, in press.
- [17] U. Haeberlen, *High Resolution NMR in Solids. Selective Averaging. Suppl. 1*, *Adv. Magn. Reson.*, Academic Press, New York 1976.
- [18] R. K. Harris, P. Reams, and K. J. Packer; *J. Chem. Soc. Dalton Trans.* **1986**, p. 1015.
- [19] M. M. Maricq and J. S. Waugh, *J. Chem. Phys.* **70**, 3300 (1979).